

Monte Carlo Simulation of Total Cross Section Measurement of ^{nat}W using Time-of-Flight Method

Jong Woon Kim^{a*}, Hyeong Il Kim^a, and Young-Ouk Lee^a

^aKorea Atomic Energy Research Institute, 111, Daedeok-daero 989 Beon-gil, Yuseong-gu, Daejeon, Korea, 34057

*Corresponding author: jwkim@kaeri.re.kr

1. Introduction

The construction of the KAERI nTOF facility is being delayed due to changes in licenses of accelerator building. The expected operating conditions of electron beam are 17 MeV, 200 kHz, and 20 ps pulse width.

In the meantime, we simulated the total cross section measurement of ^{nat}W under predicted operating conditions using MCNP6 [1]. The ^{nat}W sample is located 1 m from the source. The two neutron spectra with sample-in and -out were obtained at the detector position (7.2 m from the source) through Monte Carlo simulations.

In this paper, Monte Carlo simulation of total cross section measurement of ^{nat}W using Time-of-Flight method was performed and the simulated total cross section of ^{nat}W was compared with those of existing libraries (ENDF/B-VII.1, JENDL-4.0, and JEFF-3.2).

2. Methods and Results

2.1 Neutron Time-of-Flight Method

The Time-of-Flight (TOF) technique is a general method for determining the kinetic energy of a traveling neutron, by measuring the time it takes to fly between two fixed points whose distance is known.

A pulsed electron beam incidents to the neutron production target at t_0 , then produced neutron fly to the detector position and scored at t_s .

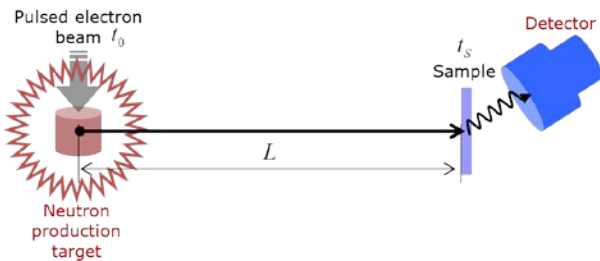


Fig. 1. The concept of neutron Time-of-Flight (TOF).

Considering time uncertainty Δt , neutron flight time t_n is calculated as Eq. (1). The speed of neutron is calculated as Eq. (2) since we know the flight path length L . The speed of neutron is converted into energy by Eq. (3).

$$t_n = (t_s - t_0) + \Delta t, \quad (1)$$

$$v \approx \frac{L}{t_n}, \quad (2)$$

$$E = m_n c^2 \left(\frac{1}{\sqrt{1 - (v/c)^2}} - 1 \right). \quad (3)$$

2.2 Neutron Attenuation

Suppose that a thick target of thickness t is placed in a mono-directional beam of flux Φ_0 and a neutron detector is located at some distance behind the target as shown in Fig. 2. It will be assumed that both the target and the detector are so small that the detector subtends a small solid angle at the target.

In this case, every neutron that has a collision in the target will be lost from the beam, and only those neutrons that do not interact will enter the detector.

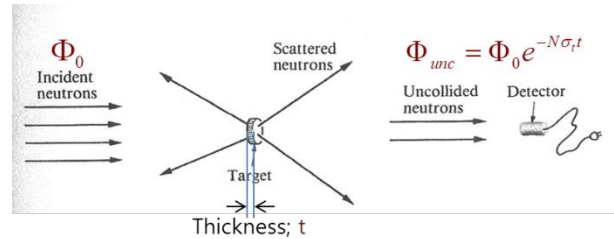


Fig. 2. Neutron attenuation (adapted from Ref. 2).

Let Φ_{unc} be the flux of the neutrons that have not collided after penetrating the distance t into the target. The flux of the uncollided beam will be decreased by the number of neutrons that have collided in the target. The flux of the uncollided neutrons thus decreases exponentially with distance inside the target. The flux of the beam of uncollided neutrons emerging from the target is then

$$\Phi_{unc} = \Phi_0 e^{-N\sigma_t t}, \quad (4)$$

where

N : atomic number density [$\#/\text{cm}^3$],

σ_t : total microscopic cross section [cm^2],

t : thickness of sample [cm].

The transmittance T [3] is defined as

$$T = \frac{\Phi_{unc}}{\Phi_0}, \quad (5)$$

and it can be rewritten as

$$T = \frac{\Phi_{unc}}{\Phi_0} = \frac{\Phi_0 e^{-N\sigma_i t}}{\Phi_0} = \frac{C_{Sample-in}}{C_{Sample-out}}, \quad (6)$$

$$\sigma_i = -\frac{1}{Nt} \ln \left(\frac{C_{Sample-in}}{C_{Sample-out}} \right), \quad (7)$$

where

$C_{Sample-in}$: detected neutron flux (sample-in),

$C_{Sample-out}$: detected neutron flux (sample-out).

$C_{Sample-in}$ and $C_{Sample-out}$ can be obtained using MCNP6 simulation, N and t are the properties of sample to measure.

2.3 Simulation

To simulate total cross section measurement, we setup geometry like Fig. 3. ^{nat}W sample and detector are located 1 m and 7.2 m from the neutron source position respectively.

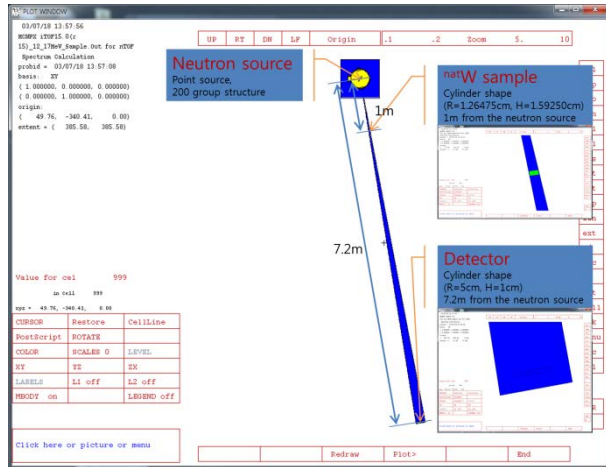


Fig. 3. The simulation layout.

KAERI nTOF facility uses a photo-neutron source that generates neutrons by injecting 17 MeV, 0.08 mA, 200 kHz pulsed electron beams into liquid lead. In this case, the yield of neutron is considerably low as shown in Table I.

Table I: Yield at the spectrum tally surface

	Electron	Photon	Neutron
Outgoing (#/one-source -particle)	$1.65225\text{E-}01$ †(0.0001)	$2.32525\text{E+}00$ †(0.0000)	$8.10926\text{E-}04$ †(0.0008)

Source particle : 1 electron/sec (@ 17 MeV)

† : relative error

To improve simulation efficiency, neutron spectrum was tallied with 200 energy group structure on the sphere ($r = 7$ cm) and shown in Fig. 4. This was used as a point source at neutron source position.

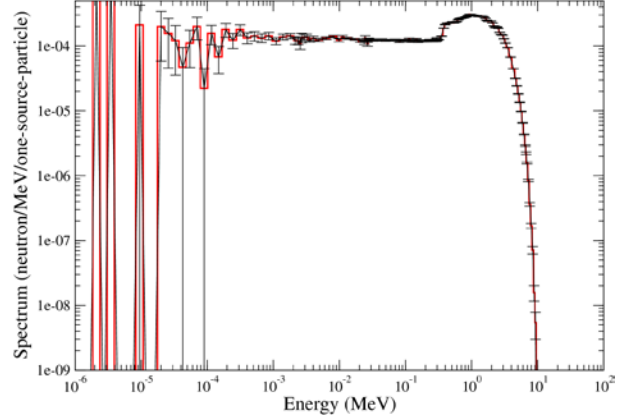


Fig. 4. Tallied neutron spectrum.

For the ^{nat}W sample, we used the identical specification that used for the total cross section measurement at the HZDR in 2013 and listed in Table II.

Table II: Specification of ^{nat}W sample

Diameter (cm)	2.52950
Height (cm)	1.59250
Mass (g)	153.2001
Density (g/cm ³)	19.1435

Two simulations were performed for the sample-in and -out cases and detailed simulation layout for each part are shown in Fig. 5.

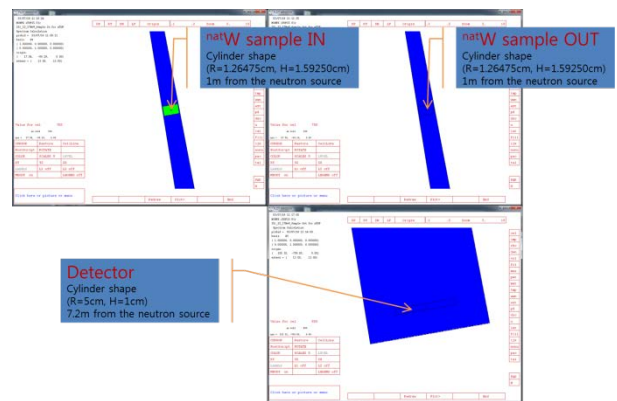


Fig. 5. Detailed simulation layout for each part. (Left top) sample-in, (Right top) sample-out, and (Right bottom) detector.

2.4 Results

Two tallied fluxes (sample-in and -out cases) were plotted in Fig. 6. As we expected, it can be seen that the

flux in the sample-in case is lower than the flux in the sample-out case.

The difference represents the amount of neutrons that the neutrons reacted with the sample and did not reach the detector.

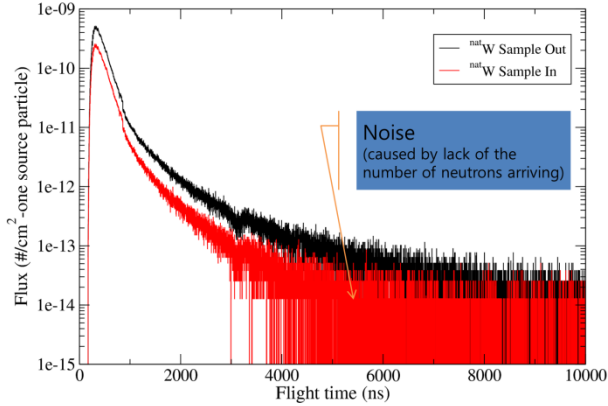


Fig. 6. The tallied neutron fluxes with flight time. (Black) sample-out and (Red) sample-in.

In Fig. 6, it can be seen that the noise is severely generated after 4,000 ns due to the lack of the number of neutrons arriving, even though we used 10^{12} neutrons in the simulation.

Considering the operating condition of the KAERI nTOF facility (0.08 mA), the number of electrons injected at the target is 4.99320×10^{14} (electron/sec) and the number of neutrons generated per second is 4.04912×10^{11} (neutron/sec) that can be calculated using the neutron yields in Table I.

Assuming that the measurement experiment lasts for several days, the neutron number used in the simulation is considerably small.

The tallied neutron fluxes are transformed into a total cross section using Eq. (7) and shown in Fig. 7.

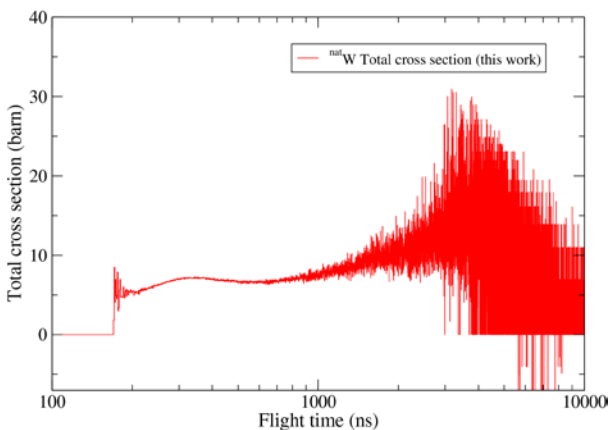


Fig. 7. The simulated total cross section of ^{nat}W with flight time.

The maximum energy of the neutron is about 9.5 MeV and the flight time of this neutron is about 170 ns. The unit of x-axis of Fig. 7 is converted from the flight time to neutron energy using Eq. (8) and the converted graph is shown in Fig. 8.

$$E_n (\text{MeV}) = 939.565 \left(\frac{1}{\sqrt{1 - 11.12650 \frac{[L(m)]^2}{[t_n(\text{ns})]^2}}} - 1 \right), \quad (8)$$

where

E_n : energy of neutron (MeV),

L : flight path length (m),

t_n : flight time (ns).

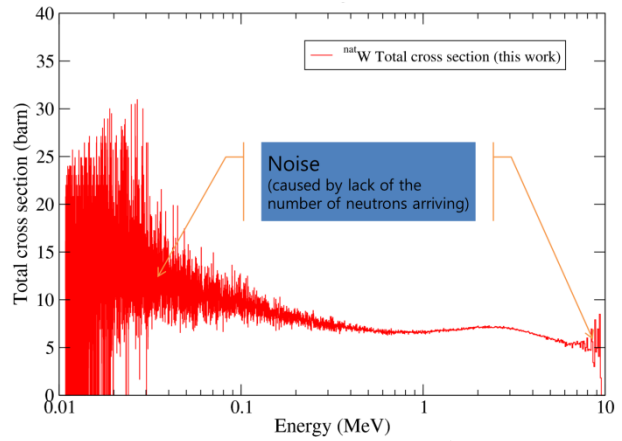


Fig. 8. The simulated total cross section of ^{nat}W with neutron energy.

To make sure that the simulations were done properly, we compared the simulated total cross sections of ^{nat}W with those of existing libraries (ENDF/B-VII.1, JEFF-3.2, and JENDL-4.0) and shown in Fig. 9.

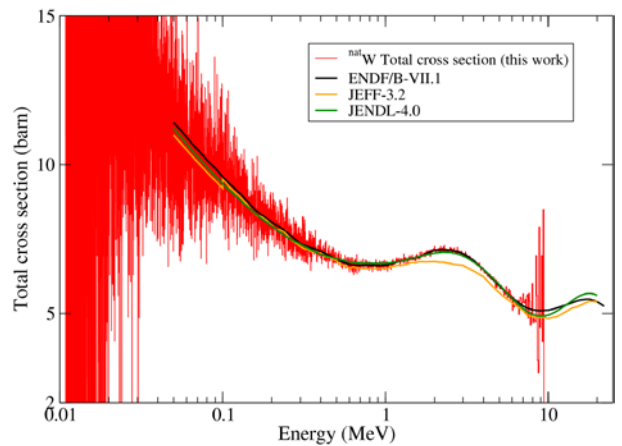


Fig. 9. The comparison of the simulated total cross section of ^{nat}W with those in the existing libraries (ENDF/B-VII.1, JEFF-3.2, and JENDL-4.0).

In the Fig. 9, the simulated total cross section of ^{nat}W is best matched with ENDF/B-VII.1 and this is a natural result because we used ENDF/B-VII.1 in the simulation.

3. Conclusions

In this paper, the ^{nat}W total cross section measurement procedure was reproduced by Monte Carlo simulation. The simulated total cross section of ^{nat}W is best matched with ENDF/B-VII.1 and this is obvious because ENDF/V-VII.1 was used in the simulation.

The detailed geometry of the KAERI nTOF facility was not reflected in this simulation, so we could not see the effect of geometry. However, in the near future, this paper will be used as a starting point to carry out the simulation including the geometry effect.

Simulating the experiments (i.e., total, inelastic scattering, and capture cross section measurements) to be carried out at KAERI nTOF facility will be a great help to the real measurement because it is possible to know in advance what arrangement of the detector is efficient, what kind of data can be obtained, and what causes noise in signal.

In real experiments, the trajectories of radiation or particles cannot be seen by eye, but they can be seen through simulation. Therefore, for researchers conducting experiments, simulation is a tool to help understand the current situation and it may prevent mistakes that can be occurred.

REFERENCES

- [1] D. B. Pelowitz, editor, "MCNP6TM USER'S Manual Version 1.0," Los Alamos National Laboratory, LA-CP-13-00634, Rev. 0, 2013.
- [2] J. R. Lamarsh, Introduction to Nuclear Engineering, 2nd Edition, Addison-Wesley Publishing Company, pp.48-51, 1983.
- [3] N. Won, et al., Establishment of Nuclear Data System – Measurements of Nuclear Data and Possibility to Construct a Nuclear Data Production Facility based on Electron Linac, KAERI/CM-455/2000, pp. 20-30, 2000.
- [4] A. Michaudon, S. Cierjacks, and R. E. Chrien, Neutron Sources for Basic Physics and Applications, An OECD/NEA Report, Neutron Physics and Nuclear Data in Science and Technology, Volume 2, pp. 83-86, 1983.